Research Square

Preprints are preliminary reports that have not undergone peer review.
They should not be considered conclusive, used to inform clinical practice,
or referenced by the media as validated information.

Mettl3-Mediated m⁶A Modification Upregulates Prmt1 to Promote Osteoblast Differentiation via the p38 MAPK Signaling Pathway

Bilan Li
Nanjing Medical University
Xinluan Jiang
Nanjing Medical University
Yunfei Ma
Nanjing Medical University
Baisheng Zhou
Nanjing Medical University
Qinyu Yuan
Nanjing Medical University
Luqi Wang
Nanjing Medical University
Qiong Guo
First Affiliated Hospital of Nanjing Medical University
Changyan Ma
cyma@njmu.edu.cn

Nanjing Medical University

Research Article

Keywords: Prmt1, Mettl3, p38, Osteoblasts, Osteoporosis

Posted Date: November 25th, 2026

DOI: https://doi.org/10.21203/rs.3.rs-11754036/v1

License: This work is licensed under a Creative Commons Attribution 4.0 International License.
Read Full License

Additional Declarations: No competing interests reported.

Abstract

Background

Bone homeostasis depends on the coordinated activities of bone-forming osteoblasts and bone-resorbing osteoclasts, and its disruption leads to osteoporosis. Protein arginine methyltransferase 1 (Prmt1) has been implicated in bone metabolism, but its role in osteoporosis remains controversial. This study investigated how Prmt1 regulates osteoblast differentiation and osteoporosis.

Methods

Osteoblast differentiation and mineralization were assessed following pharmacological inhibition of Prmt1 with AMI-1, a selective inhibitor. The effects of AMI-1 on bone loss were evaluated in ovariectomized mice. Pharmacological and molecular experiments were performed to identify the downstream signaling pathway and upstream regulator of Prmt1. Statistical significance was assessed using two-sided t tests for pairwise comparisons and analysis of variance for multigroup comparisons, as appropriate.

Results

AMI-1 suppressed osteoblast differentiation and mineralization and exacerbated osteoporosis in ovariectomized mice. Pharmacological inhibitor assays indicated that Prmt1 promotes osteoblast differentiation through the p38 mitogen-activated protein kinase pathway. Methyltransferase-like 3 (Mettl3) bound Prmt1 messenger RNA and mediated m^6A modification at site 1109 within the coding sequence, thereby upregulating Prmt1 expression.

Conclusions

Prmt1 promotes osteoblast differentiation, whereas its inhibition exacerbates estrogen deficiency-associated bone loss. Mettl3 regulates Prmt1 through RNA methylation, linking this modification to p38 signaling during osteoblast differentiation. The Mettl3–Prmt1–p38 axis is therefore a promising therapeutic target for osteoporosis, although further studies are needed to establish its clinical value.

Introduction

Osteoporosis is a major global skeletal disease closely linked to population aging, with its prevalence rising steadily worldwide. It is characterized by reduced bone mass and impaired bone microarchitecture, leading to increased bone fragility and elevated fracture susceptibility. Osteoporotic fractures cause substantial morbidity, long-term disability and increased mortality among older adults[1].

As global life expectancy continues to rise, the incidence of osteoporotic fractures is predicted to nearly double by 2050[2]. Notably, the excess mortality risk persists for years after fracture, and surviving patients frequently suffer from impaired mobility and loss of independence, thereby imposing a heavy burden on public health systems[3]. In the context of global demographic aging, the growing burden of osteoporosis underscores an urgent need for precise and targeted therapeutic strategies.

Osteoporosis is a systemic skeletal disorder characterized by reduced bone mass and impaired bone microarchitecture, which arises mainly from dysregulated balance between osteoblast-mediated bone formation and osteoclast-mediated bone resorption[4]. Key signaling pathways, including the Wnt/β-catenin, p38 MAPK and BMP/Smad pathways governing osteoblast differentiation, as well as the RANKL/OPG, NF-κB and Notch pathways regulating osteoclast activation, play pivotal roles in maintaining bone homeostasis. Dysregulation of these critical pathways is closely linked to osteoporosis progression[5, 6]. Current therapeutic interventions, such as bisphosphonates and denosumab, primarily suppress bone resorption yet fail to fully regenerate lost bone tissue. In addition, long-term use of these agents carries potential adverse events, including osteonecrosis of the jaw and atypical femoral fractures[7, 8]. Collectively, these limitations underscore the pressing need to uncover novel molecular targets capable of directly boosting osteoblastic function and restoring bone metabolic homeostasis.

Protein arginine methyltransferases (Prmts) constitute a family of enzymes that catalyze arginine methylation. This post-translational modification is essential for transcriptional regulation, signal transduction and cell lineage commitment[9, 10]. Prmt family members are categorized into two distinct subtypes. Type I enzymes mediate the formation of asymmetric dimethylarginine, whereas type II enzymes generate symmetric dimethylarginine. Prmt1 is the most abundant type I isoform within this family[11]. Prmt1 has been implicated in adipocyte and myocyte differentiation. Nevertheless, its precise roles in osteoblast biology and the pathogenesis of osteoporosis remain controversia[12–14]. Prmt1 knockdown reduces alkaline phosphatase (ALP) activity and mineralization in murine osteoblasts, supporting a pro-osteogenic function of Prmt1[15]. Conversely, Prmt1 promotes RANKL-induced osteoclastogenesis and exacerbates bone loss in ovariectomized (OVX) mice[16]. These conflicting observations highlight a critical knowledge gap regarding the exact function of Prmt1 in bone homeostasis and skeletal disease.

N^6-methyladenosine (m^6A) represents the most prevalent internal modification of eukaryotic mRNAs. It orchestrates mRNA stability, splicing and translation via the coordinated actions of m^6A writers, erasers and readers, which correspond to methyltransferases, demethylases and RNA-binding proteins, respectively[17]. Mettl3 functions as the core catalytic subunit of the m^6A writer complex and is indispensable for m^6A deposition, acting as a key modulator of stem cell differentiation[18]. Growing evidence has established a tight link between Mettl3 and bone metabolism. Mettl3 knockdown in mesenchymal stem cells (MSCs) blunts osteoblast differentiation by reducing m^6A modification of Runx2, the master transcription factor driving osteogenic differentiation[19, 20]. Clinical investigations

have also identified diminished circulating Mettl3 levels in patients with postmenopausal osteoporosis, and this reduction strongly correlates with lower bone mineral density (BMD)[21]. Notwithstanding these advances, the potential regulatory crosstalk between Mettl3 and Prmt1 in governing osteoblast function remains largely uncharacterized.

In this study, we sought to fill these critical knowledge gaps and present three major findings. First, in vivo and in vitro functional experiments demonstrated that AMI-1, a selective inhibitor of Prmt1, suppresses osteoblast differentiation and mineralization and exacerbates osteoporosis in ovariectomized (OVX) mice. Second, results from agonist and inhibitor treatments reveal that Prmt1 activates the p38 MAPK signaling cascade. Third, RNA immunoprecipitation (RIP) and m⁶A-RIP assays verify that Mettl3 directly interacts with the 1109th adenosine residue within the CDS of Prmt1 mRNA and elevates Prmt1 expression through m^6A modification. Collectively, our study uncovers the Mettl3–Prmt1–p38 axis as a previously unrecognized regulatory circuit governing osteoporosis pathogenesis, thus offering promising molecular targets to restore bone mass.

Materials and Methods

Cell culture and osteoblast differentiation

Murine preosteoblast MC3T3-E1 cells were purchased from the Cell Bank of the Chinese Academy of Sciences (Shanghai, China) and cultured in MEM Alpha (Gibco, Carlsbad, California, USA). HEK 293T cells and murine mesenchymal stem cells C3H10T1/2 were obtained from American Type Culture Collection (Manassas, Virginia, USA) and grown in DMEM (WISENT, Nanjing, China), respectively. All culture media were supplemented with 10% fetal bovine serum (WISENT, Nanjing, China) and 1% penicillin/streptomycin (NCM Biotech, Suzhou, China). For in vitro osteogenic differentiation, MC3T3-E1 and C3H10T1/2 cells were cultured in osteogenic induction medium, which consisted of basal growth medium supplemented with 50 μg/mL ascorbic acid (Sigma-Aldrich, Saint Louis, Missouri, USA), 10 mM β-glycerophosphate (Sigma-Aldrich, Saint Louis, Missouri, USA) and 10 nM dexamethasone (Sigma-Aldrich, Saint Louis, Missouri, USA).

Western blotting

Western blotting
The primary antibodies used were as follows: Prmt1 (1:1000, Cell signaling, Boston, MA, USA), Osterix (1:1000, HUABIO, Hangzhou, China), Runx2 (1:5000, HUABIO), Erk1/2 (1:1000, Proteintech, Wuhan, China), p-Erk1/2 (1:1000, Proteintech), p38 (1:2000, ABclonal, Wuhan, China), p-p38 (1:1000, ABclonal), Mettl3 (1:1000, Abcam, Cambridge, UK), Myc tag (1:3000, Proteintech), DDDDK tag (1:5000, ABclonal), HA tag (1:5000, ABclonal), and β-actin (1:10000, Proteintech).

Alkaline phosphatase (ALP) staining and alizarin red S (ARS) staining

Cells cultured in osteogenic induction medium for 7 days were fixed with 4% paraformaldehyde (PFA) at room temperature for 20 min. Alkaline phosphatase (ALP) activity was visualized using the BCIP/NBT Alkaline Phosphatase Color Development Kit (Beyotime, Shanghai, China) in accordance with the manufacturer's instructions. For alizarin red S (ARS) staining, cells underwent 14 days of osteogenic induction. After fixation with 4% paraformaldehyde for 20 min, cells were stained with 2% ARS solution (Sigma-Aldrich) at 25°C. Subsequently, non-specific staining was eliminated via PBS washing, and mineralized nodules were imaged under a light microscope.

OVX-induced osteoporosis mouse model and AMI-1 injection

All animal procedures were approved by the Institutional Animal Care and Use Committee of Nanjing Medical University (Approval No. IACUC-2107044). Female C57BL/6 mice (6 months old) were maintained in the animal facility of Nanjing Medical University. Mice were randomly assigned to three groups (n = 6 per group): (1) Sham + PBS group: sham-operated mice receiving intrafemoral marrow cavity injection of PBS; (2) OVX + PBS group: OVX mice with the marrow cavity of the femur injection of PBS; (3) OVX + AMI-1 group: OVX mice receiving intrafemoral marrow cavity injection of AMI-1, a selective small-molecule inhibitor of Prmt1, at a dose of 0.5 mg per mouse. Intrafemoral injections were initiated 1 week after surgery and administered once every two weeks for 8 consecutive weeks. Ten weeks following OVX surgery, mice were anesthetized via intraperitoneal injection of sodium pentobarbital and subsequently euthanized by cervical dislocation.

μCT analysis

Harvested mouse femurs were fixed and scanned using a SkyScan 1176 μCT system (Bruker, Karlsruhe, Germany) at a resolution of 18 μm. Three-dimensional (3D) reconstructions were generated, and subsequently, the following trabecular bone parameters were quantified: bone volume per tissue volume (BV/TV), trabecular number (Tb.N), trabecular thickness (Tb.Th), and trabecular separation (Tb.Sp).

Plasmids and shRNAs

For lentivirus-mediated overexpression, full-length cDNA encoding mouse Prmt1 was subcloned into the pLVX-puro vector, and the empty pLVX-puro vector was used as a negative control. For gene knockdown, two non-overlapping short hairpin RNA (shRNA) sequences targeting each gene were inserted into the pLKO.1-puro vector. Corresponding sequences are provided in Table S1. Point mutants (Prmt1 Luc mut 1–5) were constructed using the Mut Express II Fast Mutagenesis Kit (Vazyme), and their identities were confirmed via Sanger sequencing. Primers for plasmid construction are listed in Table S2.

Lentivirus infection and plasmid transfection

For lentiviral production, lentiviral vectors for shRNA-mediated knockdown or gene overexpression were co-transfected into HEK 293T cells along with the packaging plasmid psPAX2 and envelope plasmid pMD2.G. Lentiviral supernatants were collected 72 h after transfection and applied to infect target cells in the presence of 10 μg/mL polybrene. Subsequently, stable cell lines were selected using 5 μg/mL puromycin, and successful transduction was validated via western blotting. For transient plasmid transfection, cells were transfected with plasmids using Neofect DNA transfection reagent (Neofect, Beijing, China) in accordance with the manufacturer's instructions.

RNA sequencing

Total RNA was extracted, digested to eliminate genomic DNA contamination, and evaluated for RNA integrity. Poly(A)+ mRNA was enriched, fragmented, and subjected to library preparation. Following quality validation of the libraries, paired-end sequencing was carried out on an Illumina platform by Ribobio Co., Ltd (Guangzhou, Guangdong, China). Differentially expressed genes (DEGs) were defined as genes with $|\log_2(\text{fold change})| \geq 1$ and $P < 0.05$. Subsequently, Kyoto Encyclopedia of Genes and Genomes (KEGG) pathway enrichment analysis for DEGs was implemented using the clusterProfiler package.

Quantitative real-time PCR (qRT-PCR)

Total RNAs were isolated from cells or bone tissues using TRIzol reagent (Vazyme, Nanjing, China). For complementary DNA (cDNA) synthesis, 1 μg of total RNA was reverse-transcribed using HiScript II Q RT SuperMix for qRT-PCR (Vazyme). Real-time PCR was performed with 2×RealStar SYBR Mix (Yeason, Shanghai, China) on a real-time PCR system. Relative transcript abundance was calculated using the $2^{-\Delta\Delta Ct}$ method. Each experiment was performed in biological triplicates. Primer sequences are listed in Table S3.

RNA immunoprecipitation (RIP)-qRT-PCR assay

The RIP assay was conducted in accordance with the manufacturer's protocol for the PureBinding RNA Immunoprecipitation Kit (Jise Biotech, Guangzhou, China). Protein lysates were incubated overnight with protein A/G magnetic beads conjugated to anti-Mettl3, anti-m^6A, or IgG antibodies.

Luciferase reporter assays

The wild-type Prmt1 PCR product was cloned into the psiCHECK2 vector. Additionally, a mutant construct was generated by mutating adenine (A) to thymine (T) within the m^6A motif of Prmt1, and its PCR product was also cloned into psiCHECK2. Subsequently, these reporter constructs were individually co-transfected with pCMV-Mettl3 into HEK 293T cells. Thirty-six hours post-transfection, cell lysates were harvested using the Dual Luciferase Reporter Gene Assay Kit (Yeasen, Shanghai, China), and firefly

and Renilla luciferase activities were quantified using the Promega dual-luciferase reporter assay system.

Statistics analysis

Data are presented as mean ± standard error of the mean (SEM) from three independent experiments. Statistical analyses were performed using GraphPad Prism 10. For independent samples with normal distribution, Student's t-test was used for two-group comparisons, and one-way ANOVA was applied for comparisons among three or more groups. A p-value < 0.05 was considered statistically significant: *p < 0.05; **p < 0.01; ***p < 0.001; ^{ns}p > 0.05 indicates no significance.

Results

1. Inhibition of Prmt1 with AMI-1 suppresses osteoblast differentiation and exacerbates osteoporosis

In our prior work (manuscript under submission), we established stable cell lines with either Prmt1 overexpression or knockdown and generated osteoblast-specific Prmt1 knockout (Col1a1-Cre; $Prmt1^{-/-OB}$) mice to dissect the functional role of Prmt1 in bone metabolism. We showed that Prmt1 robustly enhances osteoblast differentiation and alleviates osteoporosis both in vitro and in vivo. To further evaluate the translational potential of Prmt1, we carried out complementary experiments to validate these observations. Specifically, MC3T3-E1 and C3H10T1/2 cells were treated with AMI-1, a selective small-molecule inhibitor of Prmt1. Western blot analyses revealed that AMI-1 treatment markedly reduced the protein abundance of osteogenic markers Runx2 and Osterix (Fig. 1A). Consistently, AMI-1 exposure diminished ALP activity and impaired extracellular matrix mineralization (Fig. 1B).

Given the established function of Prmt1 in enhancing osteoblast activity in vitro, we sought to further assess whether pharmacological inhibition of Prmt1 could aggravate osteoporosis in vivo. We generated ovariectomized (OVX) mouse models and examined the skeletal effects of AMI-1 via intrafemoral intramedullary injection (Fig. 1C). μCT analysis revealed marked bone loss in OVX mice relative to the sham-operated (Sham) group (Fig. 1D). Following AMI-1 administration, OVX mice exhibited a further reduction in bone volume/total volume (BV/TV); conversely, trabecular number (Tb.N) decreased and trabecular separation (Tb.Sp) increased additionally, whereas trabecular thickness (Tb.Th) remained unaltered (Fig. 1E). Moreover, western blot analysis showed that AMI-1 potentiated the OVX-mediated reduction in Runx2 and Osterix protein levels (Fig. 1F). Collectively, these findings demonstrate that the Prmt1 inhibitor AMI-1 suppresses osteoblast differentiation and matrix mineralization, thereby exacerbating osteoporosis.

2. Transcriptomic profiling identifies impaired p38 MAPK signaling upon Prmt1 knockdown

To pinpoint signaling pathways acting downstream of Prmt1, we conducted transcriptomic profiling in Prmt1-knockdown MC3T3-E1 cells. Differential expression analysis showed that 108 genes were upregulated, whereas 312 genes were downregulated following Prmt1 depletion (Fig. 2A and Table S4).

qRT-PCR validation confirmed reduced transcript levels of Aldh1a7, Scube3, Nrep, and Serpina3g in Prmt1-knockdown MC3T3-E1 cells (manuscript under submission). Notably, pathway enrichment analysis of differentially expressed genes (DEGs) identified enrichment of the MAPK signaling pathway in Prmt1-deficient cells (Fig. 2B).

MAPKs, a group of evolutionarily conserved serine/threonine kinases, are classified into four major subfamilies: extracellular signal-regulated kinase (ERK), p38, c-Jun amino-terminal kinase (JNK), and ERK5[21]. Subsequent pathway association analysis indicated that the DEGs were predominantly associated with the ERK and p38 signaling pathways. Accordingly, we used western blotting to evaluate total expression and phosphorylation of ERK1/2 and p38 upon Prmt1 knockdown. These data showed that Prmt1 depletion markedly reduced phosphorylated p38 (p-p38), while total p38 protein abundance remained unchanged in MC3T3-E1 and C3H10T1/2 cells. In contrast, total and phosphorylated ERK1/2 levels were unaltered (Fig. 2C).

3. Prmt1 promotes osteoblast differentiation via p38 signaling pathway

To determine whether p38 activation is required for Prmt1-driven osteoblast differentiation, Prmt1-overexpressing cells were treated with the p38 inhibitor adezmapimod. Blockade of p38 signaling abolished the Prmt1-mediated induction of Runx2 and Osterix (Fig. 3A), as well as the Prmt1-dependent increases in ALP activity and matrix mineralization (Fig. 3B). Conversely, treatment with the p38 activator DHC rescued the impaired osteogenic differentiation caused by Prmt1 knockdown, as reflected by elevated Runx2 and Osterix protein abundance and restored ALP activity and mineral deposition (Fig. 3C–D). Collectively, these data show that Prmt1 promotes osteoblast differentiation via activation of the p38 signaling pathway.

4. Mettl3 mediates the m ^{6} A modification of Prmt1 mRNA

N⁶-methyladenosine (m^6A) represents the most abundant internal RNA modification in eukaryotic cells. The m⁶A mark is dynamically deposited by the m^6A writer complex, a core methyltransferase complex composed of Mettl3, Mettl14, and Wtap. Among these components, Mettl3 functions as the primary catalytic subunit for m^6A installation. These observations raise the possibility that Mettl3-dependent m^6A modification may contribute to Prmt1 upregulation. The online prediction tool SRAMP (http://www.cuilab.cn/sramp/) predicted five putative m^6A motifs within Prmt1 mRNA (Fig. 4A). To further characterize m^6A-dependent regulators governing Prmt1 expression, Mettl3 was overexpressed in MC3T3-E1 cells. qRT-PCR analysis revealed markedly elevated Prmt1 mRNA abundance upon Mettl3 overexpression (Fig. 4B). Subsequently, RIP-qRT-PCR assays verified the direct physical interaction between Mettl3 protein and Prmt1 mRNA (Fig. 4C). Furthermore, MeRIP-qRT-PCR experiments confirmed that m^6A modification levels of Prmt1 mRNA were substantially enhanced in Mettl3-overexpressing MC3T3-E1 cells (Fig. 4D). To map the functional Mettl3-binding site on Prmt1 mRNA, we generated wild-type and mutant luciferase reporter constructs carrying the Prmt1 CDS region (Fig. 4E). Reporter assays demonstrated that Mettl3 overexpression significantly augmented luciferase activity for Prmt1-WT,

Prmt1-MUT1, Prmt1-MUT2, Prmt1-MUT3, and Prmt1-MUT4. Conversely, Mettl3 exerted no statistically detectable effect on the reporter activity of Prmt1-MUT5 (mutant 5) (Fig. 4F). Taken together, these results suggest that Mettl3 targets the adenine residue at position 1109 in the Prmt1 CDS to mediate its m^6A modification.

5. Mettl3 upregulates the expression of Prmt1 mRNA

To this end, we assessed Prmt1 transcript and protein abundance following Mettl3 overexpression or depletion in MC3T3-E1 and C3H10T1/2 cells. As illustrated in the corresponding panels, Mettl3 overexpression markedly increased Prmt1 mRNA and protein levels (Fig. 5A–C). Consistently, shRNA-mediated Mettl3 knockdown substantially reduced Prmt1 mRNA and protein abundance (Fig. 5D–F). Next, analysis of the osteoporosis dataset GSE56815 showed that both Mettl3 and Prmt1 were downregulated in osteoporotic samples, and their expression exhibited a significant positive correlation (Fig. 5G).

Discussion

This study elucidates three core mechanisms governing osteoblast differentiation and the pathogenesis of osteoporosis. First, intervention with AMI-1, a selective inhibitor of Prmt1, suppresses osteoblast differentiation and mineralization and exacerbates osteoporosis in OVX mice. Second, Prmt1 exerts its pro-osteogenic effect via activation of the p38 MAPK pathway. Third, a novel post-transcriptional regulatory axis is identified: Mettl3 directly binds to the 1109th adenosine residue within the CDS region of Prmt1 mRNA and catalyzes m^6A modification to upregulate Prmt1 expression.

Prmt1, a major arginine methyltransferase, catalyzes protein arginine methylation to govern gene expression, cell differentiation, signal transduction, and RNA metabolism[25, 26]. Prior studies have yielded conflicting findings regarding its osteogenic capacity, leaving the function of Prmt1 in bone biology poorly defined[15, 16]. Herein, using the selective Prmt1 inhibitor AMI-1 together with an in vivo OVX mouse model, we show that Prmt1 exerts a positive regulatory effect on osteoblast differentiation and matrix mineralization. Moreover, although Prmt1 is established to drive cellular differentiation in other contexts[12], our data uncover its lineage-specific function within the osteoblast lineage. Accordingly, Prmt1 may serve as a molecular switch governing osteogenic cell fate. This observation carries potential implications for the pathogenesis of age-related bone loss.

Mettl3, the core m^6A writer, modulates mRNA stability, splicing, and translation[27, 28]. By mediating site-specific m^6A deposition on mRNA, it governs stem cell differentiation, embryonic development, metabolism, and disease progression. Mettl3 has emerged as a critical regulator of bone metabolism; prior work has demonstrated that it promotes osteogenesis through m^6A-dependent regulation of Runx2 and YAP. Consistent with these observations, Mettl3 expression is reportedly diminished in patients with postmenopausal osteoporosis[19, 21, 29]. Here, our study extends the known osteogenic regulatory network of Mettl3 by identifying Prmt1 as its direct downstream target. Notably, this finding reinforces

the concept that m⁶A exerts its functions via precise, substrate-specific modifications. Furthermore, it underscores that Mettl3 orchestrates osteogenic programs through multiple downstream targets. Collectively, these results strengthen the therapeutic potential of Mettl3 for skeletal disorders[30, 31].

Collectively, our findings define the Mettl3–Prmt1–p38 axis as a previously unrecognized regulatory cascade governing osteoblast differentiation (Fig. 5H). This pathway addresses a major drawback of current anti-osteoporosis therapeutics by uncovering two candidate druggable targets: Mettl3 and Prmt1. Moving forward, future investigations may test small-molecule activators targeting Mettl3 or Prmt1 in preclinical skeletal models. In summary, this work deepens our mechanistic insight into bone metabolic regulation and offers a novel conceptual framework for developing bone-anabolic therapies.

Abbreviations

ALP: Alkaline phosphatase

AMI-1: Arginine methyltransferase inhibitor 1

ANOVA: Analysis of variance

ARS: Alizarin red S

BMD: Bone mineral density

BMP: Bone morphogenetic protein

BV/TV: Bone volume per tissue volumec

DEGs: Differentially expressed genes

MAPK: Mitogen-activated protein kinase

m⁶A (m6A): N⁶-methyladenosine

MeRIP: Methylated RNA immunoprecipitation

Mettl3: Methyltransferase-like 3

Mettl14: Methyltransferase-like 14

OVX: Ovariectomized

Prmt1: Protein arginine methyltransferase 1

RANKL: Receptor activator of nuclear factor-κB ligand

RIP: RNA immunoprecipitation

ShRNA: Short hairpin RNA

Tb.N: Trabecular number

Tb.Sp: Trabecular separation

Tb.Th: Trabecular thickness

WT: Wild type

μCT: Micro-computed tomography

Declarations

Ethics approval and consent to participate

Not applicable

Consent for publication

Not applicable

Competing interests

The authors declare no competing financial or non-financial interests.

Author Contribution

Conception and design, C. M., and Q. G.; development of methodology, B. L., X. J. and Y. M.; acquisition of data, B. L., X. J., and Y. M.; analysis and interpretation of data, B. L., X. J., Y. M., B. Z., Q. Y. and L. W.; writing, reviewing, and/or revision of the manuscript, C. M. and Q. G.; Funding acquisition, C. M.. All authors have read and approved the final manuscript.

Acknowledgements

This study was supported by grants from the National Natural Science Foundation of China (No. 82373058 and 82072484).

Data availability

Data will be made available on request.

References

1. Naso CM, Lin SY, Song G, Xue H (2025) Time trend analysis of osteoporosis prevalence among adults 50 years of age and older in the USA, 2005–2018. Osteoporos Int 36(3):547–554
2. Wang H, Zhao Y, Liu Q, Jiang Z, Zhou H, Wang Q (2025) Global burden of low bone mineral density related fractures in pre- and post-menopausal women from 1990 to 2021, with projections to 2050. Osteoporos Int 36(9):1593–1605
3. Ye C, Schousboe JT, Morin SN, Lix LM, Leslie WD (2022) Time since prior fracture affects mortality at the time of clinical assessment: a registry-based cohort study. Osteoporos Int 33(6):1257–1264
4. Rizzoli R, Chevalley T (2024) Nutrition and Osteoporosis Prevention. Curr Osteoporos Rep 22(6):515–522
5. Hu L, Chen W, Qian A, Li YP (2024) Wnt/β-catenin signaling components and mechanisms in bone formation, homeostasis, and disease. Bone Res 12(1):39
6. Kim JM, Lin C, Stavre Z, Greenblatt MB, Shim JH (2020) Osteoblast-Osteoclast Communication and Bone Homeostasis. Cells. ;9(9)
7. Li M, Ge Z, Zhang B, Sun L, Wang Z, Zou T et al (2024) Efficacy and safety of teriparatide vs. bisphosphonates and denosumab vs. bisphosphonates in osteoporosis not previously treated with bisphosphonates: a systematic review and meta-analysis of randomized controlled trials. Arch Osteoporos 19(1):89
8. Reid IR, Billington EO (2022) Drug therapy for osteoporosis in older adults. Lancet 399(10329):1080–1092
9. Guccione E, Richard S (2019) The regulation, functions and clinical relevance of arginine methylation. Nat Rev Mol Cell Biol 20(10):642–657
10. Zhu Y, Xia T, Chen DQ, Xiong X, Shi L, Zuo Y et al (2024) Promising role of protein arginine methyltransferases in overcoming anti-cancer drug resistance. Drug Resist Updat 72:101016
11. Thiebaut C, Eve L, Poulard C, Le Romancer M (2021) Structure, Activity, and Function of PRMT1. Life (Basel). ;11(11)
12. Choi S, Choi D, Lee YK, Ahn SH, Seong JK, Chi SW et al (2021) Depletion of Prmt1 in Adipocytes Impairs Glucose Homeostasis in Diet-Induced Obesity. Diabetes 70(8):1664–1678
13. Zhu Q, Wang D, Liang F, Tong X, Liang Z, Wang X et al (2022) Protein arginine methyltransferase PRMT1 promotes adipogenesis by modulating transcription factors C/EBPβ and PPARγ. J Biol Chem 298(9):102309
14. Tran TTV, Jeong Y, Kim S, Yeom JE, Lee J, Lee W et al (2025) PRMT1 Ablation in Endothelial Cells Causes Endothelial Dysfunction and Aggravates COPD Attributable to Dysregulated NF-κB Signaling. Adv Sci (Weinh) 12(19):e2411514
15. Ye H, Cao L, Jackson-Weaver O, Zheng L, Gou Y (2023) PRMT1-mediated arginine methylation promotes postnatal calvaria bone formation through BMP-Smad signaling. Bone 176:116887
16. Choi JH, Jang AR, Kim DI, Park MJ, Lim SK, Kim MS et al (2018) PRMT1 mediates RANKL-induced osteoclastogenesis and contributes to bone loss in ovariectomized mice. Exp Mol Med 50(8):1–15

17. Jiang X, Liu B, Nie Z, Duan L, Xiong Q, Jin Z et al (2021) The role of m6A modification in the biological functions and diseases. Signal Transduct Target Ther 6(1):74
18. Zeng C, Huang W, Li Y, Weng H (2020) Roles of METTL3 in cancer: mechanisms and therapeutic targeting. J Hematol Oncol 13(1):117
19. Zhou S, Zhang G, Wang K, Yang Z, Tan Y (2024) METTL3 potentiates osteogenic differentiation of bone marrow mesenchymal stem cells via IGF2BP1/m6A/RUNX2. Oral Dis 30(3):1313–1321
20. Tian C, Huang Y, Li Q, Feng Z, Xu Q (2019) Mettl3 Regulates Osteogenic Differentiation and Alternative Splicing of Vegfa in Bone Marrow Mesenchymal Stem Cells. Int J Mol Sci. ;20(3)
21. Wang Y, Chen Y, Xiao H, Liu Z, Liu X, Feng Z et al (2024) METTL3-mediated m6A modification increases Hspa1a stability to inhibit osteoblast aging. Cell Death Discov 10(1):155
22. Hwang JH, Park YS, Kim HS, Kim DH, Lee SH, Lee CH et al (2023) Yam-derived exosome-like nanovesicles stimulate osteoblast formation and prevent osteoporosis in mice. J Control Release 355:184–198
23. Wang Z, Wang Y, Tang Y, Guo X, Gao Q, Shao Y et al (2025) Sodium Benzoate Inhibits Osteoblast Differentiation and Accelerates Bone Loss by Regulating the FGF2/p38/RUNX2 Pathway. J Agric Food Chem 73(22):13891–13901
24. Xu Y, Song M, Hong Z, Chen W, Zhang Q, Zhou J et al (2023) The N6-methyladenosine METTL3 regulates tumorigenesis and glycolysis by mediating m6A methylation of the tumor suppressor LATS1 in breast cancer. J Exp Clin Cancer Res 42(1):10
25. Yao B, Gui T, Zeng X, Deng Y, Wang Z, Wang Y et al (2021) PRMT1-mediated H4R3me2a recruits SMARCA4 to promote colorectal cancer progression by enhancing EGFR signaling. Genome Med 13(1):58
26. Walton J, Ng ASN, Arevalo K, Apostoli A, Meens J, Karamboulas C et al (2024) PRMT1 inhibition perturbs RNA metabolism and induces DNA damage in clear cell renal cell carcinoma. Nat Commun 15(1):8232
27. Poh HX, Mirza AH, Pickering BF, Jaffrey SR (2022) Alternative splicing of METTL3 explains apparently METTL3-independent m6A modifications in mRNA. PLoS Biol 20(7):e3001683
28. Wei X, Huo Y, Pi J, Gao Y, Rao S, He M et al (2022) METTL3 preferentially enhances non-m(6)A translation of epigenetic factors and promotes tumourigenesis. Nat Cell Biol 24(8):1278–1290
29. Sun X, Meng X, Piao Y, Dong S, Dong Q (2024) METTL3 promotes the osteogenic differentiation of human periodontal ligament cells by increasing YAP activity via IGF2BP1 and YTHDF1-mediated m(6)A modification. J Periodontal Res 59(5):1017–1030
30. Roundtree IA, Evans ME, Pan T, He C (2017) Dynamic RNA Modifications in Gene Expression Regulation. Cell 169(7):1187–1200
31. Chen L, Zhang C, Ma W, Huang J, Zhao Y, Liu H (2022) METTL3-mediated m6A modification stabilizes TERRA and maintains telomere stability. Nucleic Acids Res 50(20):11619–11634

Figures

Fig.1 Inhibition of Prmt1 with AMI-1 suppresses osteoblast differentiation and exacerbates osteoporosis

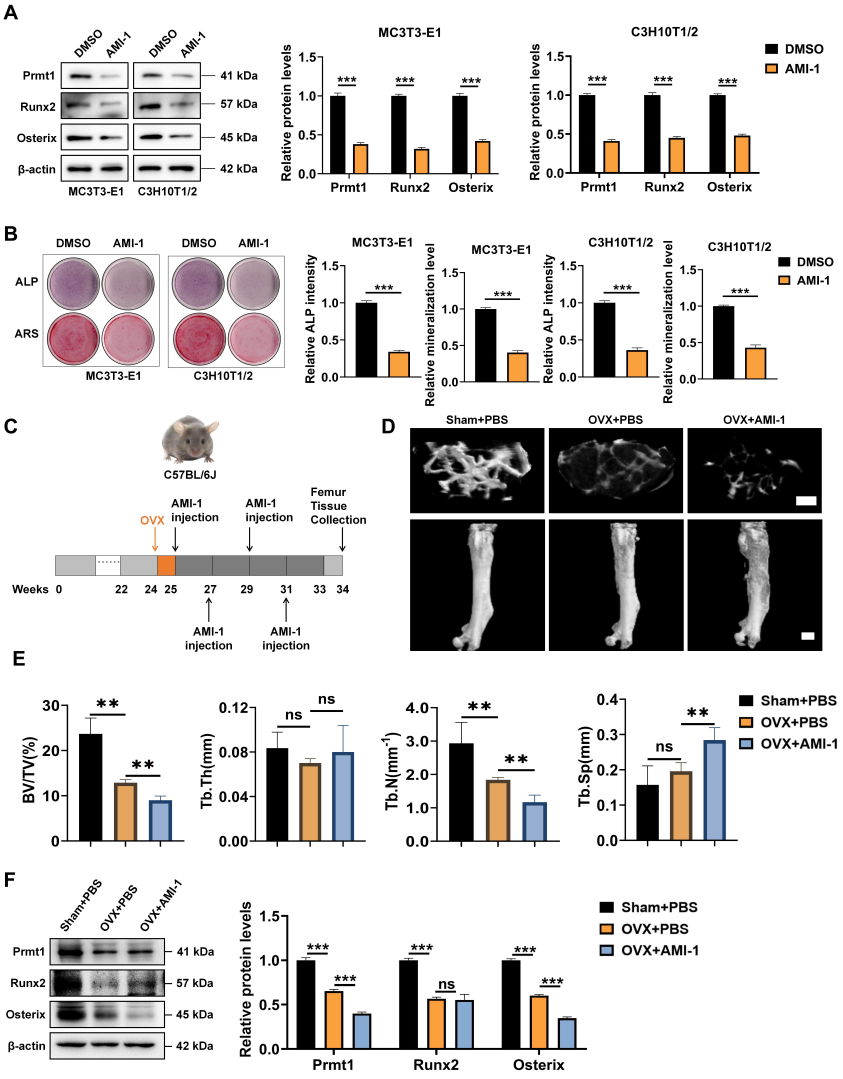


Figure 1

Inhibition of Prmt1 with AMI-1 suppresses osteoblast differentiation and exacerbates osteoporosis

MC3T3-E1 and C3H10T1/2 cells were cultured with or without 10 μM AMI-1 (a selective inhibitor of Prmt1) for 48 h, followed by osteogenic induction in differentiation medium. A. Western blot analysis of Prmt1, Runx2 and Osterix in MC3T3-E1 and C3H10T1/2 cells upon the treatment with AMI-1.

Densitometric quantification is presented in the right panel. B. ALP and ARS staining in MC3T3-E1 and C3H10T1/2 cells upon the treatment with AMI-1. Densitometric quantification of staining intensity is presented in the right panel. C. Schematic diagram illustrating the experimental procedure (n = 6 mice per group). D. Representative μCT images of femurs from the indicated groups of mice. Scale bar = 500 μm. E. Histomorphometric analysis of distal femurs from the indicated groups of mice. Parameters include BV/TV, Tb.Th, Tb.N, and Tb.Sp. F. Western blot analysis of Prmt1, Runx2 and Osterix in the femurs from the indicated mice. Densitometric quantification is presented in the right panel.

Fig.2 Transcriptomic profiling identifies impaired p38 MAPK signaling upon Prmt1 knockdown

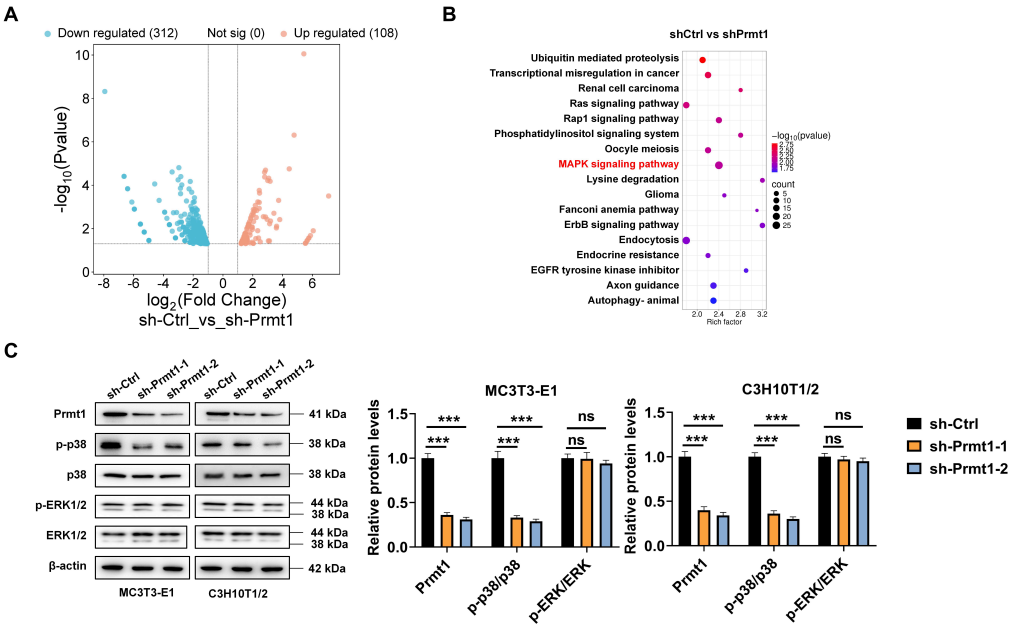


Figure 2

Transcriptomic profiling identifies impaired p38 MAPK signaling upon Prmt1 knockdown

A. Volcano plot showing the global gene expression profile in Prmt1-knockdown MC3T3-E1 cells. B. KEGG pathway enrichment analysis to identify significantly enriched signaling pathways in Prmt1-knockdown MC3T3-E1 cells. C. Western blot analysis of p38 MAPK, p-p38 MAPK, Erk1/2 MAPK and p-Erk1/2 MAPK protein levels in Prmt1 knockdown MC3T3-E1 and C3H10T1/2 cells. Densitometric quantification is presented in the right panel.

Fig.3 Prmt1 promotes osteoblast differentiation via p38 signaling pathway

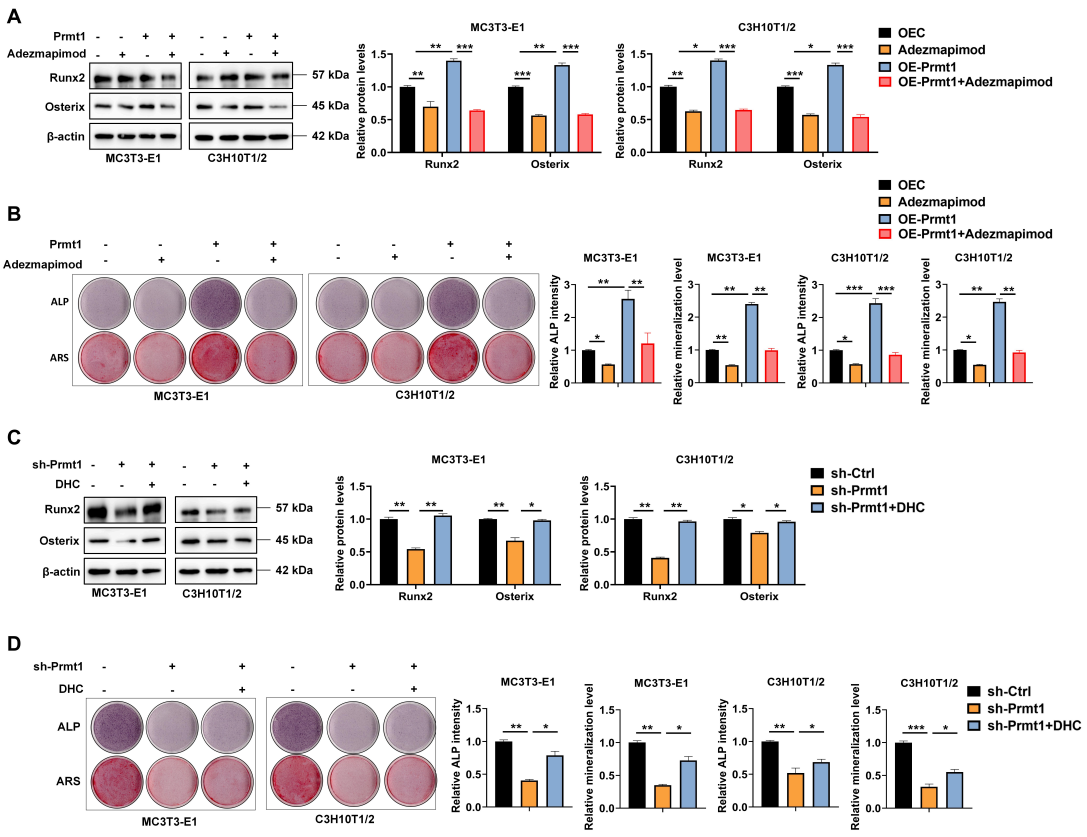


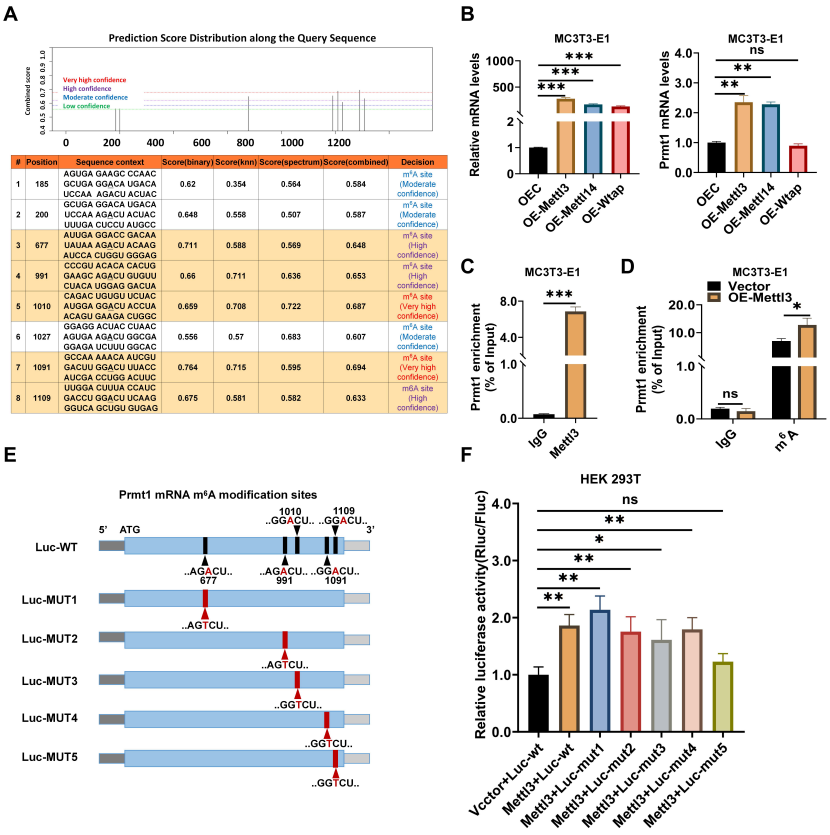
Figure 3

Prmt1 promotes osteoblast differentiation via p38 signaling pathway

A. Western blot analysis of Runx2 and Osterix in Prmt1-overexpressing MC3T3-E1 and C3H10T1/2 cells following treatment with Adezmapimod (a p38 inhibitor). Densitometric quantification is presented in the right panel. B. ALP and ARS staining of Prmt1-overexpressing MC3T3-E1 and C3H10T1/2 cells treated

with Adezmapimod.Densitometric quantification of staining intensity is presented in the right panel. C. Western blot analysis of Runx2 and Osterix in MC3T3-E1 and C3H10T1/2 cells following exposure to DHC (a p38 activator). Densitometric quantification is presented in the right panel. D. ALP and ARS staining of Prmt1-overexpressing cells treated with DHC. Densitometric quantification of staining intensity is presented in the right panel.

Fig.4 Mettl3 mediates the m^{6}A modification of Prmt1 mRNA



#	Position	Sequence context	Score(binary)	Score(knn)	Score(spectrum)	Score(combined)	Decision
1	185	AGUGA GAAGC CCAAC GCUGA GGACA UGACA UCCAA AGACU ACUAC	0.62	0.354	0.564	0.584	m^{6}A site (Moderate confidence)
2	200	GCUGA GGACA UGACA UCCAA AGACU ACUAC UUUGA CUCCU AUGCC	0.648	0.558	0.507	0.587	m^{6}A site (Moderate confidence)
3	677	AUUGA GGACC GACAA UAUAA AGACU ACAAG AUCCA CUGGU GGGAG	0.711	0.588	0.569	0.648	m^{6}A site (High confidence)
4	991	CCCGU ACACA CACUG GAAGC AGACU GUGUU CUACA UGGAG GACUA	0.66	0.711	0.636	0.653	m^{6}A site (High confidence)
5	1010	CAGAC UGUGU UCUAC AUGGA GGACU ACCUA ACAGU GAAGA CUGGC	0.659	0.708	0.722	0.687	m^{6}A site (Very high confidence)
6	1027	GGAGG ACUAC CUAAC AGUGA AGACU GGCGA GGAGA UCUUU GGCAC	0.556	0.57	0.683	0.607	m^{6}A site (Moderate confidence)
7	1091	GCCAA AAACA AUCGU GACUU GGACU UUACC AUCGA CCUGG ACUUC	0.764	0.715	0.595	0.694	m^{6}A site (Very high confidence)
8	1109	UUGGA CUUUA CCAUC GACCU GGACU UCAAG GGUCA GCUGU GUGAG	0.675	0.581	0.582	0.633	m6A site (High confidence)

Figure 4

Mettl3 mediates the m^{6}A modification of Prmt1 mRNA

A. The m^{6}A modification sites in Prmt1 were predicted with the SRAMP online tool (http://www.cuilab.cn/sramp). B. qRT-PCR analysis of m^{6}A writers (Mettl3, Mettl14 and Wtap) overexpression efficiency and Prmt1 expression level in MC3T3-E1 cells transfected with Mettl3, Mettl14 or Wtap overexpression constructs. C. RIP-qRT-PCR assays demonstrated that Mettl3 could interact with Prmt1. D. The m^{6}A level of Prmt1 was evaluated by MeRIP-qRT-PCR in MC3T3-E1 cells transfected with or without Mettl3 expression plasmid. E. Schematic diagram of the wild-type and mutated Prmt1 reporter plasmid constructions. F. Luciferase reporter assays were performed in HEK 293T cells after transfection of wild-type or mutated Prmt1 reporter plasmid together with Mettl3 expression plasmid (n = 3 for each group).

Fig.5 Mettl3 upregulates the expression of Prmt1.

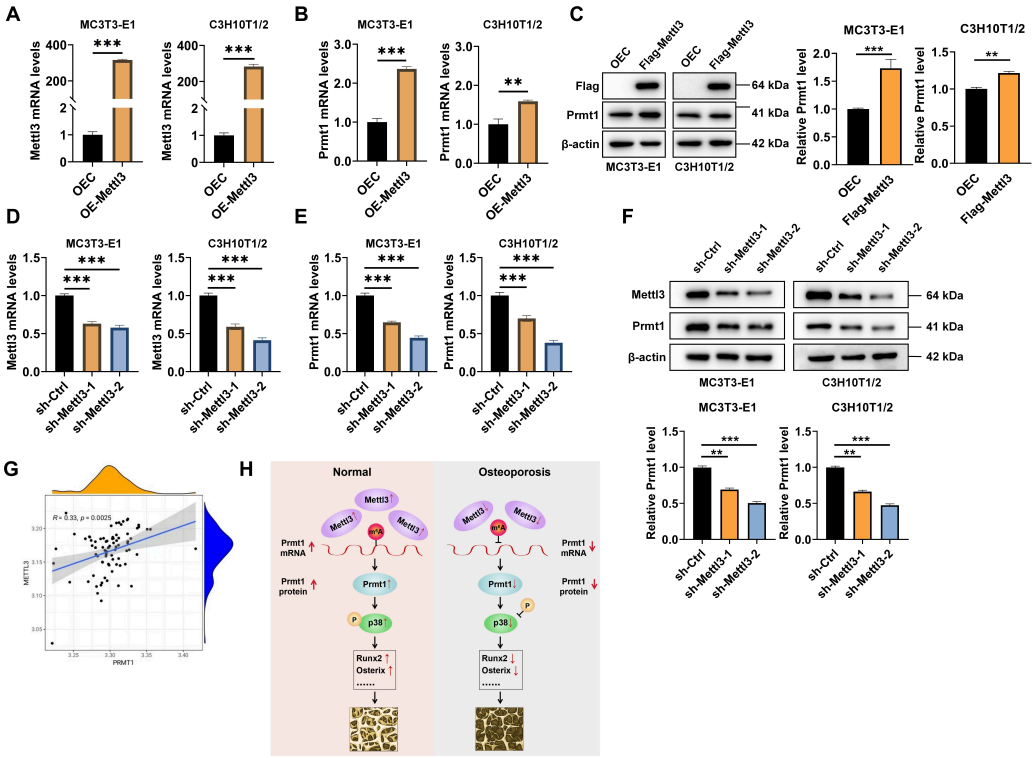


Figure 5

Mettl3 upregulates the expression of Prmt1 mRNA

A. qRT-PCR analysis of Mettl3 expression level in MC3T3-E1 and C3H10T1/2 cells transfected with Mettl3 expression plasmid. B. qRT-PCR analysis of Prmt1 expression level in MC3T3-E1 and C3H10T1/2 cells transfected with Mettl3 expression plasmid. C. Western blot analysis of Mettl3 and Prmt1

expression level in MC3T3-E1 and C3H10T1/2 cells transfected with Mettl3 expression plasmid. Densitometric quantification is presented in the right panel. D. qRT-PCR analysis of Mettl3 expression level in MC3T3-E1 and C3H10T1/2 cells transfected with shScramble or sh-Mettl3 plasmids. E. Western blot analysis of Prmt1 expression level in MC3T3-E1 and C3H10T1/2 cells transfected with shScramble or sh-Mettl3 plasmids. F. Western blot analysis of Mettl3 and Prmt1 expression level in MC3T3-E1 and C3H10T1/2 cells transfected with shScramble or sh-Mettl3 plasmids. Densitometric quantification is presented in the lower panel. G. Associations between METTL3 and PRMT1 in osteoporosis database GSE56815 (n = 80) were assessed by Pearson correlation analysis. H. Proposed model illustrating the regulatory mechanism of the Mettl3-Prmt1-p38 axis in osteogenesis and bone formation.

Supplementary Files

This is a list of supplementary files associated with this preprint. Click to download.

- TableS13.docx
- TableS4.xls